On the Observed Characteristics of Quasi-Geostrophic Turbulence

JULIA NOGUES PAEGLE AND JAN PAEGLE

Department of Meteorology, University of Utah, Salt Lake City 84112

(Manuscript received 2 May 1975; in revised form 2 September 1975)

ABSTRACT

Observed perturbation kinetic and available energy are presented for a region about 3000 km on a side to study the horizontal homogeneity and general characteristics of geostrophic motions. Frequency spectral analysis is used to determine the dependence of these characteristics on time scales. For all time scales considered the perturbation energies display horizontal inhomogeneities, but these are less pronounced for shorter time scales. For time scales smaller than 4 days the spectra of horizontal kinetic and available potential energies decrease with increasing frequency, and approximately fit power laws with exponents between -2 to -3.5, depending on location. The frequency spectra for geostrophic vertical velocities are markedly different for different climatic locations. The frequency spectra are related to one-dimensional wavenumber spectra by introducing suitable transformation of variables. The results obtained for the higher end of these spectra are interpreted in terms of those predicted by Charney for quasi-geostrophic turbulence.

1. Introduction

In this paper we present the results obtained from one point frequency spectra of geostrophic wind components, 200 mb thicknesses and 2-level quasi-geostrophic vertical motions for the winter season. Two-point cross spectral analysis of heights at several pressure levels are also presented. The principal goals are i) to ascertain the statistical characteristics of geostrophic motion, ii) the degree of homogeneity and isotropy in these statistics, and iii) the propagation characteristics of the phenomena.

The Eulerian frequency spectra are useful tools for the purposes outlined above, since they allow determination of spatial variations of the spectral characteristics and this bears directly on homogeneity, an important property of turbulent flows. For certain scales frequency spectra can be interpreted in terms of wavenumber spectra. Such a correspondence is important because most theories dealing with predictability (Lorenz, 1969) relate to spectral slopes in wavenumber space. Much of this theory relates to the higher wavenumber range of synoptic scale waves which are difficult to resolve with the current data coverage, which has large voids over oceans. Such problems are not as pronounced for frequency spectra. The data available for frequency spectra over continents is generally influenced by nonuniform underlying conditions (Paegle and Paegle, 1975, hereafter referred as I; Kao *et al.*, 1974). Thus, it is of considerable interest to ascertain the extent to which spectral characteristics of geostrophic motions are affected, whether wavenumber-frequency transformation of spectra are possible, and for which scales such transformation might be workable.

The spectra of this study are computed on a region about 3000 km on a side (Fig. 1) in the vicinity of the Rocky Mountains. All atmospheric variables were obtained from the heights at 850, 700, 500, and 300 mb for this region, for three winter seasons (December, January, and February, 1965–1967) from the National Meteorological Center analysis. The nonuniform lower boundary conditions over the region of study might be expected to produce inhomogeneities in the flow statistics. These are most obvious in the contribution to the variances from different frequency ranges presented in Section 2. Section 3 presents spectral results at single points. The frequency spectra suggest slopes that approach a -3 power law, both for horizontal winds and available potential energy for periods less than four days. A -3 power law in wavenumber spectra would be consistent with the theory of geostrophic turbulence presented by Charney (1971) and corresponds to a critical slope in the predictability theory presented by Lorenz (1969). For the case of non-dispersive, non-amplifying waves, frequency and wavenumber spectra should show similar slopes. Section 4 discusses the frequency ranges for which the waves are predicted to be essentially non-dispersive and stable by a linearized quasi-geostrophic model over flat terrain. Observed wave propagation, inferred from two-point cross spectra of the data, tend to support the results of this analysis for certain levels and latitudes.

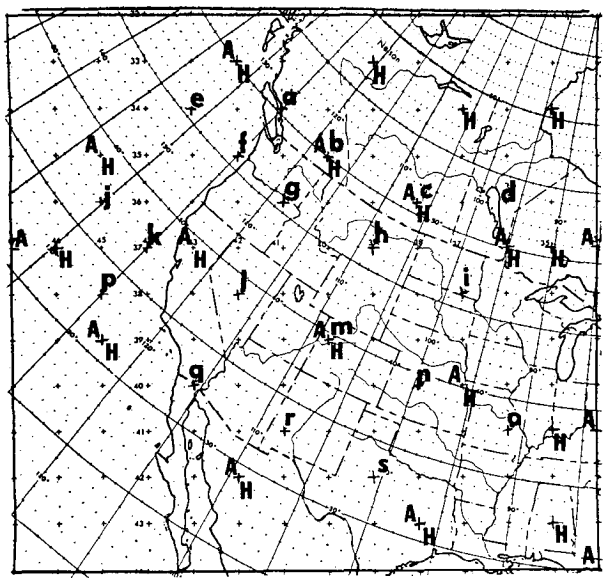

FIG. 1. 14×13 grid (+). Horizontal, and available potential energy spectra obtained at points marked H, and A, respectively. Vertical energy spectra obtained at points a) through s).

2. Turbulent kinetic and available potential energies

a. General discussion

Recently, Kao *et al.* (1974) discussed the effect of a mountain barrier on the turbulent and mean atmospheric motions as obtained from wind observations at various levels. In I, the effect of the Rocky Mountains upon the kinematics of the motion for the same grid as the one used here is discussed. The present paper represents an extension of this study to turbulent kinetic and available potential energy, as well as quasi-geostrophic vertical motion. The turbulent available potential energy is estimated at two levels from the thickness between 700 and 500 mb, and between 500 and 300 mb.

Large scale geostrophic flow is characterized by being essentially horizontal. This is apparent in that the kinetic energy associated with the horizontal motion is much larger than that associated with the vertical motion. Nevertheless, vertical motions are important since they are responsible for the transformation from potential to kinetic energy required to drive geostrophic disturbances, and are directly associated with cloudiness and precipitation. We have included spectral computations of vertical velocities obtained from a two-level quasi-geostrophic model as described in Paegle and Keirulff (1974). This is of interest to reveal the characteristics of large scale vertical turbulent kinetic energy and to obtain a quantitative measure of the degree of two-dimensionality of geostrophic flow for different time scales.

Figure 2 presents total time variances which may be regarded as the perturbation contribution to horizontal and vertical kinetic energy and available potential energy per unit mass multiplied by 2. The latter quantity is depicted only at the lowest level for which it was computed, because this is the layer associated with the greatest baroclinicity. The values for the available potential energy (P) were obtained in units of energy per unit mass by multiplying the spectral analysis of thicknesses by the appropriate factor $g^2S(p)^{-1}(\Delta p)^{-2}$, where g is the acceleration of gravity, $S(p)=2.2\times10^{-12}$ m^4 s^2 gram^{-2} (consistent with Gates, 1961) and $\Delta p=200$ mb. These results are in agreement with those reported by Oort (1964).

The horizontal geostrophic kinetic energy increases markedly with height in the lower half of the atmosphere. Both the vertical and meridional kinetic energies have maximum values in the northwestern sector of the grid associated with the semipermanent zone of low pressure over the Gulf of Alaska. This region is characterized by large variabilities of heights (I) in conjunction with the passage and development of baroclinic synoptic systems in this area. There is a minimum of zonal kinetic energy (k_u) just to the lee of the mountains which tilts toward the west with height. A relative maximum of meridional kinetic energy (k_v) is found at the lee of the mountains at 850 mb. The turbulent vertical kinetic energies per unit mass (k_w) are 10^5 to 10^6 times smaller than the horizontal kinetic energies. Similar to k_u, there is a minimum of k_w over and partially to the lee of the mountains.

b. Contributions from small, intermediate and long time scales

It is of interest to separate the contribution from different time scales to k_u, k_v, k_w, and P. Small, intermediate and long time scales are defined in Table 1.

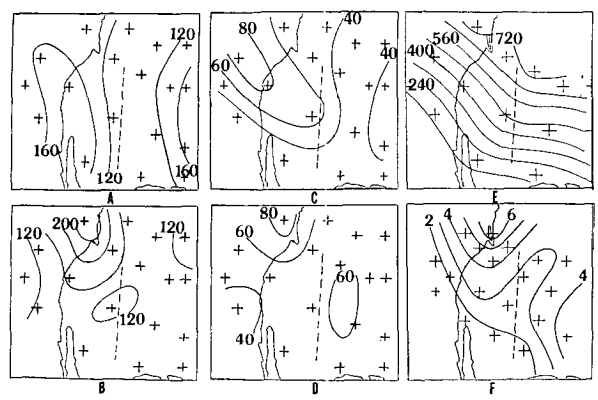

FIG. 2. Perturbation energies. Zonal kinetic energy at 500 mb (A), and 850 mb (C); meridional kinetic energy at 500 mb (B) and 850 mb (D), available potential energy obtained from 700–500 mb thicknesses (E); vertical kinetic energy (F). A through D in m^2/s^2; F in cm^2/s^2. The dashed line indicates the approximate location of the eastern slope of the Rocky Mountains.

TABLE 1. Definition of time scales.

T = time scale in days	
If $1 \leq T \leq 2$	small
$2 < T \leq 8$	intermediate
$8 < T$	long

The energy of the horizontal flow for different period ranges is shown in Figs. 3 and 4. This decomposition shows some interesting features. The overall westward maximum of k_u revealed in Fig. 2 at 500 mb is due to separate contributions from a maximum of k_u for long scales (k_{uL}) located at the northwestern sector of the grid and another separate maximum located near the southwestern sector of the grid for intermediate scales (k_{uI}). It is interesting to note the large contributions from k_{vI} at the lee of the mountains at both levels. In (I) we offered one possible explanation for this effect. Figure 5 shows the pattern of P_L to be similar to that previously shown for P, with a pronounced minimum over the Rockies and maximum partially over and to the lee of the mountains. Of these features, only the maximum over and to the east of the mountains is evident for the intermediate scales. The small time scale presents a larger degree of homogeneity than either of the two other time scales.

Figure 6 shows that the general pattern for the vertical kinetic energy is approximately established by the intermediate and long time scales. For k_{ws} there is a general increase with latitude for all longitudes. There is a general decrease of k_w toward the subtropics. The ratio between the variance of vertical velocity and the variance of the horizontal motion is a measure of the horizontality of the motion. This ratio is shown in Table 2 for several latitudes. It can be seen that the horizontality of the motion decreases with decreasing time scales and it increases with decreasing latitude for all time scales.

The variation with longitude of the perturbation kinetic energies is summarized in Table 3. This table shows an interesting shift from long to small time scales in the contribution to k_w from the west to the east of the area.

In this section we have discussed the overall characteristics of the perturbation kinetic and available potential energies over a variety of geographical locations, their contribution from three time scales and the degree of inhomogeneity that exists. Next, we will describe the turbulence spectra with greater emphasis on spectral slopes.

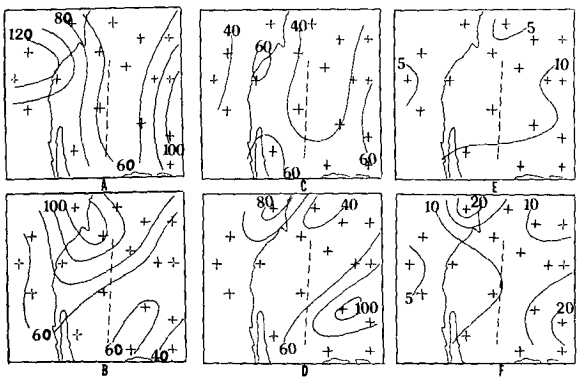

FIG. 3. Contributions to the time variance of the zonal wind, A, C, and E; and the meridional wind, B, D and F; from long, intermediate, and small time scales, respectively, in m²/s² at 500 mb. Dashed line as in Fig. 2.

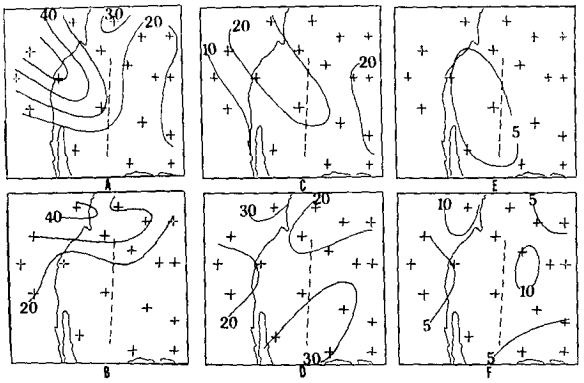

FIG. 4. Same as Fig. 3 for 850 mb.

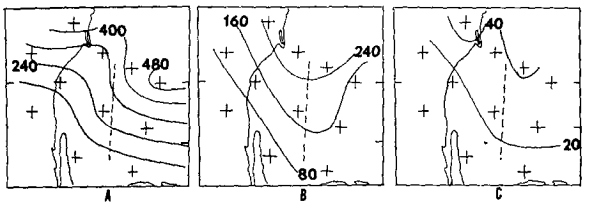

FIG. 5. Same as Fig. 3 for the available potential energy obtained from the 500–700 mb thicknesses in m²/s².

3. Spectral analysis

Figure 7 represents the spectra for the geostrophic wind components for the 15 grid points labelled H on Fig. 1. For periods of approximately 4 days or less, the spectra decreases with frequency in an approximate linear way in a log-log representation. The slopes vary between −2.0 to about −3.5 for different locations. The southermost latitudes present a tendency for

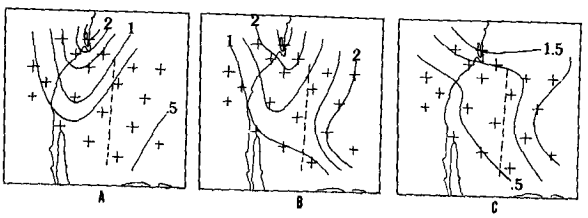

FIG. 6. Same as Fig. 3 for the vertical kinetic energy at 500 mb in cm²/s².

TABLE 2. Wind variance averaged over all longitudes considered and ratio between vertical wind and horizontal wind variances, 500 mb.

Latitude	$\bar{k}_w \times 10^{-4}$ m²/s²	$\bar{k}_u + \bar{k}_v$ m²/s	$\bar{k}_w/(\bar{k}_u+\bar{k}_v)$ $\times 10^{-6}$	$\bar{k}_{wL}/(\bar{k}_{uL}+\bar{k}_{vL})$ $\times 10^{-6}$	$\bar{k}_{wI}/(\bar{k}_{uI}+\bar{k}_{vI})$ $\times 10^{-6}$	$\bar{k}_{ws}/(\bar{k}_{us}+\bar{k}_{vs})$ $\times 10^{-6}$
50°	4.15	287.4	1.4	0.65	1.8	5.3
40°	2.88	301.0	0.9	0.34	1.3	3.8
30°	1.60	269.4	0.6	0.21	0.82	2.1

smaller slopes than higher latitudes, as already implied in Figs. 3 and 4. This is expected since the shape of the spectra is determined mainly by the existing energy at long time scales. An increase of slope with latitude was also found by Kao and Wendell (1970) in their frequency analysis of non-geostrophic winds.

The spectral results for P obtained at grid points labelled A in Fig. 1 are shown in Fig. 8. The P spectra are in general smoother than those for k_u and k_v. Many of these spectra seem to fit a slope of -3 for time scales smaller than 4 days. There seems to be a tendency for P spectra slopes to be smaller at the southernmost latitude, similar to the k_u and k_v spectra.

Figure 9 shows the spectra for k_w for grid points given in Fig. 1. The main feature of the spectra is the shift from large spectral values from low to intermediate and high frequency bands from the west to the east of the grid. The maximum values at the eastern grid points are found at periods of about 3 days. *A priori* confidence bands for the obtained spectra are also given in these figures. These bands can be used to test for expected individual spectral features.

The slopes discussed in this section can be related directly to those of the wavenumber spectra when certain assumptions are made. In the next section we discuss those assumptions and the time scale for which they are valid, according to our observational analysis.

4. Frequency and wavenumber spectra

The purpose of this section is to relate a one dimensional frequency spectra at a fixed point $\Phi_1(\omega)$ to a one dimensional instantaneous wavenumber spectra $\Phi_2(k)$. Here ω represents the frequency and k the magnitude of a horizontal wavenumber vector of direction α. Given the current data set it may be necessary to assume such transformation. The alternative assumption is that data interpolation in data void regions is sufficiently good to compute accurate wavenumber spectra in the higher wavenumbers of synoptic scales. At this point it is difficult to say which assumption is better justified and we have chosen the former as one possible interpretation of our results.

TABLE 3. Latitudinally averaged kinetic energies, 500 mb.

	About	132°W	121°W	107°W	95°W
in m²/s²	$\bar{k}_{uL}$	107.7	79.2	59.25	66.75
	$\bar{k}_{uI}$	38.7	44.5	42.5	45.0
	$\bar{k}_{us}$	7.0	6.5	8.5	9.0
	$\bar{k}_{vL}$	86.7	96.7	74.0	58.5
	$\bar{k}_{vI}$	62.7	44.7	50.7	79.0
	$\bar{k}_{vs}$	10.7	10.2	10.7	12.7
	About	125°W	117°W	108°W	98°W
in 10^{-4} m²/s²	k_{wL}	1.32	0.92	0.35	0.25
	k_{wI}	1.42	1.65	1.17	1.7
	k_{ws}	0.8	0.7	0.78	1.2

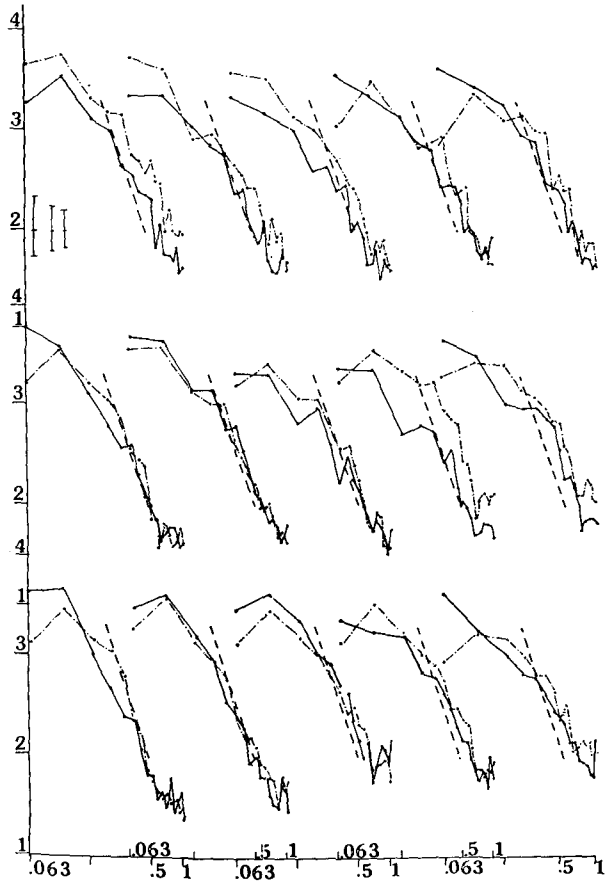

FIG. 7. Frequency spectra for the zonal (solid line) and meridional (dash-dot line) geostrophic wind components in log-log scale at 500 mb. Ordinate represents the powers of 10 to obtain the spectra in (m²/s²) Day, abscissa is frequency in cycles per day. The dashed line has a slope of -3. Confidence bands at the 1%, 5% and 10% confidence level (30 degrees of freedom) are drawn in the upper left corner.

There seems to be some discussion about the proper parameter to use to obtain such transformation (Julian, 1971; Vinnichenko, 1970). Some ambiguities are clarified by considering the transformation of variables proposed by Kinsman (1965), which can be applied whenever a well defined frequency-wavenumber dispersion relationship exists.

If $f(k,\alpha,\omega)$ represents the three dimensional wavenumber-frequency spectra, then

$$F(k,\omega)=\int_0^{2\pi} f(k,\alpha,\omega)k\,d\alpha \tag{1}$$

represents the contribution from all directions to the spectra of k and ω. If a dispersion relationship of the form $\omega=\omega(k,\alpha)$ is satisfied, then

$$F(k,\omega')=F(\omega')\delta(k-k'), \tag{2}$$

where δ represents the Dirac delta function.

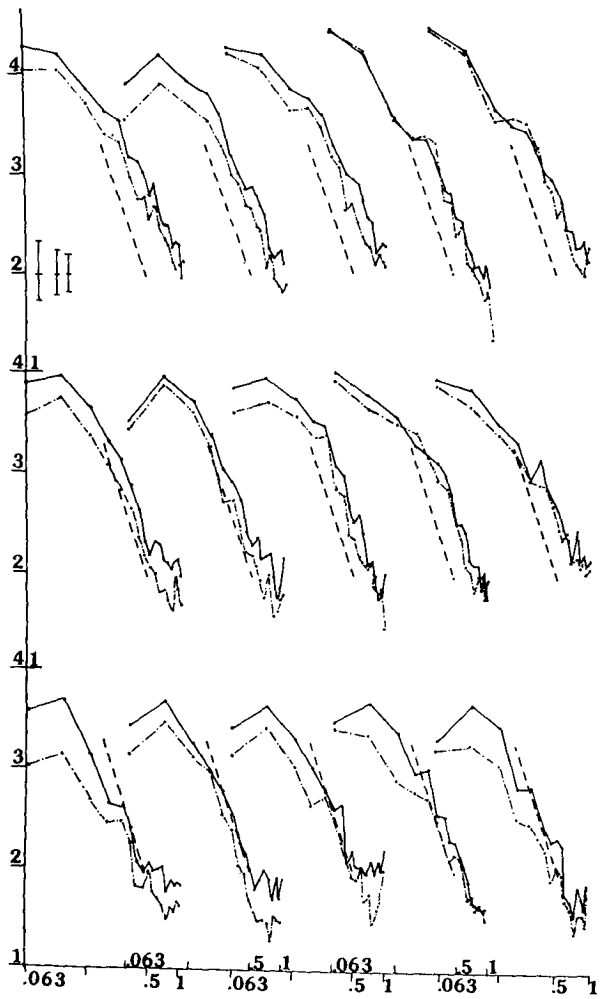

FIG. 8. Same as Fig. 7 for 700–500 mb thickness (solid line) and 500–300 mb thickness (dash-dot line) in m² Day.

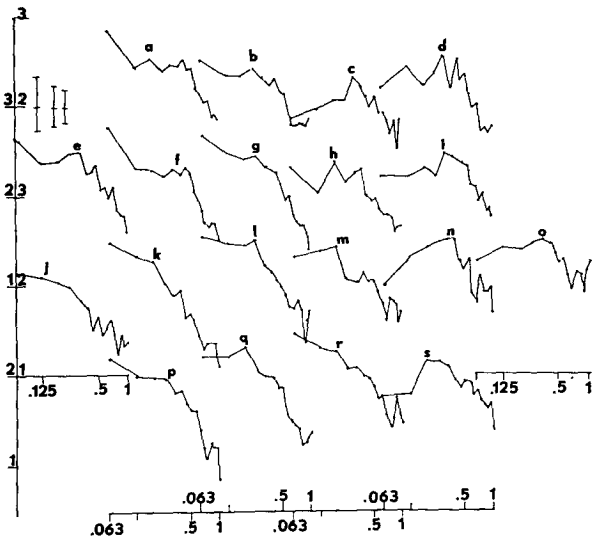

FIG. 9. Same as Fig. 7 for vertical velocities at 500 mb in (mm²/s²) Day. The letters are location identifiers corresponding to those of Fig. 1.

Since

$$\Phi_1(\omega)=\int_0^{\infty} F\,dk'$$

and

$$\Phi_2(k)=\int_0^{\infty} F\,d\omega'$$

it follows that

$$\Phi_2(k)=\int_0^{\infty} F\delta(k-k')G\,dk; \tag{3}$$

where $G=d\omega'/dk'$ and

$$\Phi_1(\omega)=\int_0^{\infty} F\delta(k'-k)dk'. \tag{4}$$

The integrals in (3) and (4) are non-zero only for $k=k'$ and

$$\Phi_2(k)=G\Phi_1(\omega). \tag{5}$$

The concern in this paper is with geostrophic motions and thus we selected a simple two level linearized quasi-geostrophic model to determine the dispersion relation (Phillips, 1954). The disturbances are of the form $\cos(k_y y)\exp[ik_x(x-ct)]$ superimposed on a zonal flow U. The latitudinal extent of the wave is given by π/k_y. Following Phillips, (1954):

$$C_{1,2}=U-\beta n^{-2}+\beta\lambda^2[2n^2(n^2+\lambda^2)]^{-1}[1\pm A], \tag{6}$$

where

$A=[1-4\bar{u}_T^2 n^4(\lambda^4-n^4)\beta^{-2}\lambda^{-4}]^{\frac{1}{2}}$

C is the phase speed

β is the beta parameter

$n^2=k_x^2+k_y^2$

TABLE 4. Phases in degrees for height between (a) 118°W and 106°W; (b) 106°W and 95°W; (c) 95°W and 85°W; (d) 122°W and 107°W; (e) 107°W and 96°W; (f) 96°W and 84°W; (g) 123°W and 109°W; (h) 109°W and 96°W; (i) 96°W and 83°W at approximately the same latitude. Values in parentheses are phase confidence bands at the 10% significance levels (Koopmans, 1974). Phases with coherences smaller than .390 (critical value to test the hypothesis of no-coherence at this significance level) have been included for completeness. These values have blanks between parentheses.

MB	0.250 cycles per day			0.5 cycles per day		
			About 50°N			
300	53 (±12)	53 (±15)	59 (±15)	98 (±21)	96 (±17)	90 (±15)
500	46 (±15)	45 (±17)	47 (±18)	94 (±23)	98 ( )	77 (±21)
700	17 (±20)	25 (±17)	28 (±13)	53 (±25)	93 ( )	72 (±19)
850	2 (±15)	37 (±15)	34 (±10)	58 (±26)	87 (±37)	76 (±21)
	(a)	(b)	(c)	(a)	(b)	(c)
			About 40°N			
300	98 (±38)	61 (±17)	112 (±44)	157 ( )	139 (±23)	110 (±15)
500	77 ( )	55 (±19)	103 ( )	158 (±39)	126 (±20)	122 (±18)
700	39 ( )	41 (±34)	65 ( )	136 ( )	140 ( )	127 (±31)
850	49 ( )	9 (±32)	14 (±46)	151 (±48)	81 ( )	117 (±27)
	(d)	(e)	(f)	(d)	(e)	(f)
			About 30°N			
300	111 (±30)	95 (±20)	108 (±30)	108 ( )	150 (±23)	147 (±26)
500	104 (±33)	92 (±19)	115 (±33)	156 ( )	138 (±22)	146 (±19)
700	66 ( )	65 (±26)	122 ( )	163 ( )	123 (±46)	161 (±27)
850	21 ( )	33 (±27)	123 ( )	76 ( )	125 (±47)	140 (±47)
	(g)	(h)	(i)	(g)	(h)	(i)

$\lambda^2=f^2/C_G^2$

f is the Coriolis parameter

C_G is the phase speed of interval gravity waves and $\bar{u}_T$ is the zonally averaged longitudinal thermal wind. From (6)

$$G=C+k_x\frac{\partial C}{\partial k_x} \tag{7}$$

is the group velocity for this wave.

Figure 10 depicts the group velocities obtained from (7) as a function of k_x for typically observed atmospheric values for stable waves and for wavenumbers larger than those of unstable waves. For $\bar{u}_T \leq 10$ m/s and fairly stable conditions, the dependence of G upon k is very weak for wavelengths smaller than about 3500 km (about wavenumber 7 at 50° of latitude). For other values this statement should be modified as indicated by Fig. 10.

If G does not depend on k, then $G=C$ and all waves propagate at the same phase speed. This is qualitatively similar to Taylor's hypothesis of frozen turbulence where all waves move with the velocity U of the mean flow, as might in general be assumed for smaller scales. Now (5) can be used to obtain relationships between $\Phi_1(\omega)$ and $\Phi_9(k)$ by considering either $G=C$ from (6) or $G=U$ depending upon the horizontal scales of interest. For the case of $G \doteq 10$ m/s, a wavelength of 3.500 km would correspond to a period of about 4 days. Charney (1971) predicts a k^{-3} dependence for horizontal kinetic and available potential energy spectra for turbulence scales small compared to the baroclinic excitation scales. Similar slopes have been observed (Kao, 1970; Kao and Wendell, 1970; and others) for wavenumbers larger than 7.

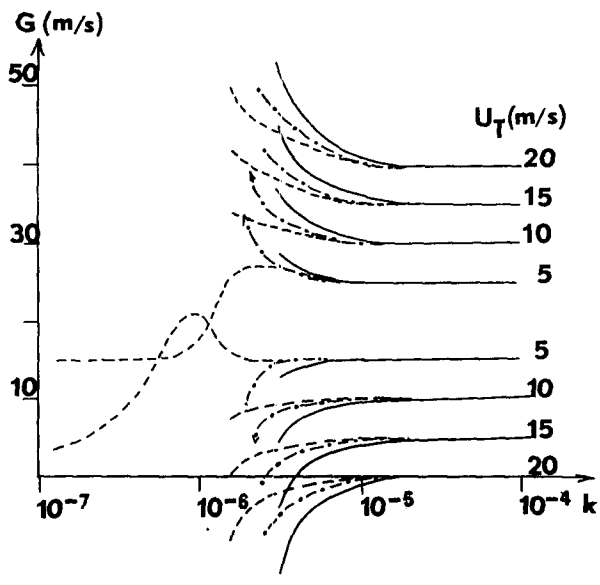

FIG. 10. Group velocity vs k_x (radians per meter) for stable waves for $C_G=35$ m/s (solid line), 45 m/s (dash-dot line), and 60 m/s (dashed line).

Periods smaller than 2 days come closer than longer periods to satisfying the conditions of local isotropy and homogeneity required by Charney's theory, as discussed in the previous section. If a given frequency is associated with the same wavenumber, the phase propagation should be uniform across the grid. The variability of the propagation rate is indicated in Table 4. For a frequency band centered on periods of 2 days, the phase differences obtained from a two point cross spectra analysis at approximately the same latitude are fairly constant for all points presented, above the mountain range, for pressure levels 700 mb and above. For the other frequency band presented, larger differences in the phase field appear. Caution should be exercised in interpreting these results due to the large confidence bands at some points. The relatively uniform phases across the grid for large frequencies suggest that a given frequency is associated with the same local wavelength across the region under investigation. For the upper level data at 50°N and some points at 40°N, the phases for .5 day^{-1} are roughly twice those at .250. This may partially justify the assumption of a simple linear wavenumber-frequency dependence.

To interpret the results for the vertical kinetic energy spectra, we consider that

$$W = -f_0 N^{-2}\left(\frac{\partial}{\partial t} + \mathbf{V}\cdot\nabla\right)\psi_z, \tag{8}$$

where all the notation is that of Charney (1971). Since the local time thickness changes are smaller than the advective changes, if the flow is to be maintained geostrophic and hydrostatic as is the case for synoptic scale motions, it follows that

$$W \doteq -\frac{f_0}{N^2}\mathbf{V}\cdot\nabla\psi_z.$$

For the small non-dispersive scales previously discussed we can further write

$$W \doteq -\frac{f_0}{N^2}Uk\psi_z,$$

and then

$$\langle W^2\rangle \doteq \frac{f_0^2}{N^4}U^2k^2\langle\psi_z^2\rangle = \frac{U^2k^2}{N^2}P,$$

where $\langle\ \rangle$ refers to an ensemble average. For geostrophic turbulence, Charney (1971) has shown that P is proportional to k^{-3} and thus we would expect $\langle w^2\rangle$ to follow a k^{-1} law, or for non-dispersive waves the frequency spectra should follow an ω^{-1} law.

Merilees and Warn (1972) have shown that, for a two-level model, P should be expected to be proportional to k^{-5} for small scales, which would indicate a k^{-3} law for $\langle W^2\rangle$ and an ω^{-3} law for non-dispersive waves. The vertical velocity spectra presented in Fig. 9 generally decays with ω for periods smaller than 3 days. The slopes of these spectra for these time scales are, in general, between -1 to -3.

5. Summary and conclusions

Observed kinetic and available potential energies have been presented to study the general statistical characteristics and homogeneity of geostrophic motion, as well as the dependence of these characteristics upon time scales.

The vertical kinetic energy revealed that the horizontality of the quasi-geostrophic motion decreases with decreasing time scales and increases with decreasing latitude. There is also a shift from long to small time scales in the contribution to the vertical kinetic energy from the west to the east of the region under study.

For all time scales considered the perturbation energies display horizontal inhomogeneities which are less pronounced for the smaller time scales. Some of these features can be attributed to the influence of the lower boundary.

For time scales smaller than 4 days the spectra of horizontal kinetic and available potential energies decrease with increasing frequency, and approximately fit power laws with exponents between -2 to -3.5, depending on location. The frequency spectra for vertical velocities in general decrease with increasing frequency for western grid points while maxima at about 3 days are found in the lee side of the mountains.

The frequency spectra can be related to one-dimensional wavenumber spectra by introducing suitable transformation of variables. For the case of non-dispersive waves such transformation reduces to a very simple form, and the results in the frequency spectra can be interpreted in terms of those observed and predicted for the one-dimensional wavenumber spectra.

REFERENCES

Charney, J. G., 1971: Geostrophic turbulence. *J. Atmos. Sci.*, **28**, 1087–1093.

Kao, S. K., 1970: Wavenumber-frequency spectra of temperature in the free atmosphere. *J. Atmos. Sci.*, **27**, 1000–1007.

——, J. N. Paegle, and W. E. Normington, 1974: Mountain effect on the motion in the atmosphere's boundary layer. *Boundary Layer Meteor.*, **7**, 501–512.

—— and L. L. Wendell, 1970: The kinetic energy of the large scale atmospheric motion in wavenumber-frequency space. *J. Atmos. Sci.*, **27**, 359–375.

Kinsman, B., 1965: *Wind Waves.* New Jersey, Prentice-Hall (see pp. 341–342).

Koopmans, L. H., 1974: *The Spectral Analysis of Time Series.* Academic Press (see pp. 285–287)

Gates, W. L., 1961: Static stability measures in the atmosphere. *J. Meteor.*, **18**, 526–533.

Julian, P. R., 1971: Some aspects of variance spectra of synoptic scale tropospheric wind components in midlatitudes and in the tropics. *Mon. Wea. Rev.*, **12**, 954–965

Lorenz, E. N., 1969: The predictability of a flow which possesses many scales of motion. *Tellus*, **21**, 289–307.

Meriless, P. E., and T. Warn, 1972: The resolution implications of geostrophic turbulence. *J. Atmos. Sci.*, **29**, 990–991.

Oort, A. H., 1964: On estimates of the atmosphere energy cycle. *Mon. Wea. Rev.*, **92**, 483–492.

Paegle, J. N., and L. P. Keirulff, 1974: Synoptic climatology of 500 mb winter flow types. *J. Appl. Meteor.*, **13**, 205–212.

Paegle, J. N., and J. Paegle, 1975: On the frequency spectra of atmospheric motions in the vicinity of a mountain barrier. Accepted for publication in the *J. Atmos. Sci.*

Phillips, N., 1954: Energy transformations and meridional circulations associated with simple baroclinic waves in a two-level quasi-geostrophic model. *Tellus*, **6**, 273–286.

Vinnichenko, N. K., 1970: The kinetic energy spectrum in the free atmosphere—1 second to 5 years. *Tellus*, **22**, 158–166.